Article

Locating Potential Groundwater Pathways in a Fringing Reef Using Continuous Electrical Resistivity Profiling

Matthew W. Becker, Francine M. Cason and Benjamin Hagedorn

Topic

Monitoring Inland Water Quality and Ecological Status

Edited by
Prof. Dr. Fei Xiao, Dr. Mengyuan Zhu and Dr. Lingling Zhu

Article

Locating Potential Groundwater Pathways in a Fringing Reef Using Continuous Electrical Resistivity Profiling

Matthew W. Becker *, Francine M. Cason and Benjamin Hagedorn

Department of Earth Science, California State University Long Beach, 1250 Bellflower Blvd., Long Beach, CA 90815, USA; klaus.hagedorn@csulb.edu (B.H.)
* Correspondence: matt.becker@csulb.edu

Abstract: Groundwater discharge from high tropical islands can have a significant influence on the biochemistry of reef ecosystems. Recent studies have suggested that a portion of groundwater may underflow the reefs to be discharged, either through the reef flat or toward the periphery of the reef system. Understanding of this potential discharge process is limited by the characterization of subsurface reef structures in these environments. A geophysical method was used in this study to profile the reef surrounding the high volcanic island of Mo'orea, French Polynesia. Boat-towed continuous resistivity profiling (CRP) revealed electrically resistive features at about 10–15 m depth, ranging in width from 30 to 200 m. These features were repeatable in duplicate survey lines, but resolution was limited by current-channeling through the seawater column. Anomalous resistivity could represent the occurrence of freshened porewater confined within the reef, but a change in porosity due to secondary cementation cannot be ruled out. Groundwater-freshened reef porewater has been observed near-shore on Mo'orea and suggested elsewhere using similar geophysical surveys, but synthetic models conducted as part of this study demonstrate that CRP alone is insufficient to draw these conclusions. These CRP surveys suggest reefs surrounding high islands may harbor pathways for terrestrial groundwater flow, but invasive sampling is required to demonstrate the role of groundwater in terrestrial runoff.

Keywords: submarine groundwater discharge; electrical resistivity; continuous resistivity profiling; tropical reefs; near-surface geophysics; carbonate geology

1. Introduction

The terrestrial–marine interface on volcanic islands has long been recognized as a critical zone for understanding marine ecosystems. unoff from islands provides critical nutrients that support reef ecosystems [1], affect the morphology of reef construction [2], and can degrade reef habitat through pollution [3–5]. Volcanic basalts are typically of very high permeability, transferring much of the runoff from surface water to groundwater. Consequently, the impact of submarine groundwater discharge (SGD) to reef systems has become an important area of study in the past decade.

The recognition that freshwater spring discharge into marine coasts is as old as human history [5]. At the margin of volcanic islands faults, joints, and lava tubes facilitate highly prolific and measurable discharges of submarine groundwater [6–8]. The hydrogeology of diffuse and low-flow discharges from islands are more enigmatic. SGD in these systems has proven to be more difficult to characterize and nearly impossible to quantify. Tracers such as radon and radium [9,10], dissolved silica [11,12], dissolved organic matter [13], temperature [6,14] have been used to help quantify discharge, but the tremendous dilution due to large volumes of moving coastal waters has limited the accuracy of these methods. In addition, because freshwater floats on seawater it can be difficult to obtain representative water samples to measure these tracers. Geophysical methods, particularly electrical resistivity profiling, have shown that one reason SGD is difficult to quantify in volcanic-reef

interfaces is because some fraction of the discharge may underflow the reef and emerge further offshore [10,15,16]. Understanding this critical zone, consequently, requires a better understanding of subreef structure and permeability.
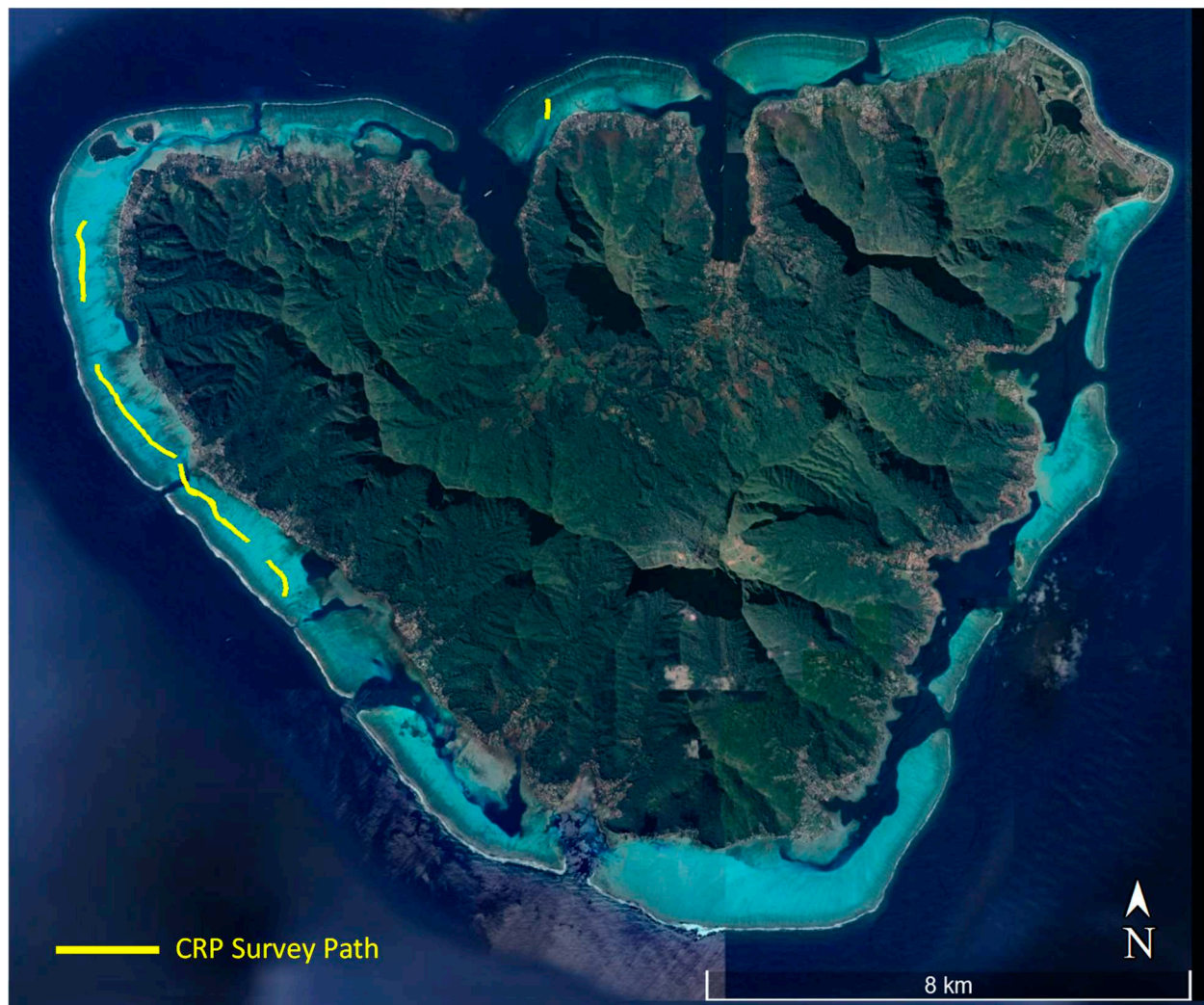
Carbonate exposures are common on volcanic islands. In some cases, carbonate completely covers (e.g., Bermuda) or fringes volcanic deposits in raised platforms (e.g., Guam) depending upon its tectonic history [17]. These carbonate islands are distinctly different than high volcanic islands with fringing reefs and/or barrier reef systems where carbonate deposits do not drive recharge but may influence the behavior of runoff at the coast. The Mo'ili'ili karst that underlies the some of the city of Honolulu in Hawai'i is a prominent example of a Pleistocene carbonate platform that forms a dendritic drainage system with offshore springs [18]. More commonly, volcanic islands are surrounded by submerged carbonate reef systems with only a very limited exposure at the shoreline. The movement of groundwater through these marine carbonates is much more difficult to identify and characterize where it exists, requiring invasive (e.g., coring) or non-invasive (e.g., geophysical) investigations in marine environments.

Even though the building and expansion of reefs surrounding volcanic islands has been well understood in broad terms since the mid nineteenth century [19], details of the subsurface structure, particularly the shallow subsurface structure, of fringing and barrier reefs are lacking. There are very few examples of tropical coral reefs in which sufficient high-resolution shallow cores have been collected to interpolate sub-reef sedimentation and lithology [2,20]. Reefs of Pacific low elevation carbonate atolls have been better characterized than those surrounding high volcanic islands, because studies have been conducted in the vicinity of cold war nuclear testing in the pacific [21,22] and because atolls are so reliant on groundwater [23–26]. Consequently, most models of fringing reef permeability are extrapolated from exposed carbonate systems or from investigations of groundwater atolls.

Here we investigate the hypothesis that groundwater runoff from high volcanic islands extends below fringing reef systems. Sub-reef groundwater movement was documented using piezometers on Davies Reef, a mid-shelf reef in the Great Barrier reef of Australia [27,28]. On shorelines dominated by carbonate deposits, off-shore karstic submarine springs are well documented [29–32]. Examples on reefs fringing volcanic islands are few, however. Electrical resistivity profiles collected in a shallow lagoon of the reef surrounding the high island of Rarotonga, Cook Islands, revealed resistive features that correlated in some points with salinity, temperature, ^{222}Rn, and ^{223,224,226}Ra measurements that suggested the leakage of groundwater [15,16]. Our previous work on Mo'orea suggested groundwater confined below the fringing reef within 100 m of shore [10]. The purpose of the current investigation was to identify confined groundwater confined beneath the reef over greater distances from shore and, if identified, to characterize the spatial distribution of groundwater. We discuss the potential movement of groundwater below the reef in terms of what is currently understood about shallow reef structure and permeability.

Geology and Sedimentary Facies of Fringing Reefs

Reefs which build out from the terrestrial landform with limited lagoons are considered fringing reefs, while reefs with extensive lagoons dividing the forereef and the shoreline are considered barrier reefs. Some islands, such as Mo'orea, may include both fringing- and barrier-reef environments (Figure 1). Darwin [19] divided fringing reefs into three zones that are still referenced today: forereef, reef crest, and backreef, progressing from ocean to land. Here, we focus on the backreef, which is typically the most extensive region of high island reefs. The backreef surface consists of coral communities and reef debris, which are typically incised by channels and may include lagoons. The focus of our investigation along the western margin of Mo'orea is classified as a fringing reef with a shallow lagoon.

Figure 1. Map of CRP surveys collected from the reefs of Mo'orea, French Polynesia (lat. 17.5, long 149.8); 2021 boat-towed electrical resistivity continuous resistivity profiling (CRP) surveys are shown in yellow. Profiles and their geographic coordinates are provided in Supplementary Material.

Reefs are almost entirely biogenic, composed of skeletal carbonate sediments produced by marine organisms. Reef growth is the result of a complex process involving calcification, breakdown, deposition, transport, cementation, dissolution, and re-cementation. The primary control on growth rate is the availability of a water column above the reef structure typically referred to as "accommodation space". However, rates are also impacted by chemistry, temperature, wave behavior, and terrestrial sediment load.

The primary reef framework is constructed from hard corals which are deposited on the seafloor. Detritus from this primary growth is bound by coraline algae and en-crusting corals, among other biota, during secondary growth. Erosion may be physical (e.g., wave and current action), or biological (e.g., due to grazing and boring organisms). Erosive processes leave voids which are often infilled by fine carbonate sediment and mud. Cementation occurs as aragonite or magnesium calcite are precipitated from seawater. Cementation results in lithification of originally loose coral sediments and thus has the effect of drastically reducing the porosity of the reef strata.

Reef growth is linked to terrestrial water sources through sediment loading and carbon and nutrient fluxes. Sediments impede the growth of corals as do large discharges of fresh water from stream outlets [2]. The relationship between reef construction and groundwater discharge is less clear. In cases where groundwater discharge is large and focused, say from lava tubes or karstic springs, reef growth can be inhibited. Reef biochemistry can be altered

by groundwater discharge which can impact reef health [33], but effects on reef accretion rates have not be identified. It has been suggested that reef pinnacles occur in zones of localized sub-reef water discharge, but there is little direct evidence that this is a general occurrence [34].

Due to subaerial exposure of carbonate during the Pleistocene low sea-stands, Holocene strata typically overlie Pleistocene strata unconformably. The Holocene/Pleistocene boundary can, therefore, be spatially complex with rough topography, as revealed by marine seismic profiles [35–37]. The Hawaiian islands of Maui, Lanai, and Molokai, for example, were once interconnected by limestone bridges, the topography of which is still expressed on the seafloor [38]. As sea levels fell through the Holocene, Pleistocene carbonate platforms about volcanic islands were exposed and karstified. This topography exerts a strong influence over the geomorphology of modern reefs [2,20,39]. Due to karstification, Pleistocene strata are known to be of much higher permeability than overlying Holocene strata on atolls. In reference to groundwater aquifers on atolls, the interface between Pleistocene limestone and Holocene sediments is called the "Thurber discontinuity" [23,40].

Drilling and coring operations have been used to characterize subsurface stratification of tropical reefs, mostly on atolls and particularly those with a history of nuclear testing. On Entewetak atoll, Marshall Islands, a site of nuclear testing by the United States, three deep and twenty-one shallow cores were collected on islets (motu) [21]. Chevalier [41] reports that a hundred shallow drillings between 15 and 30 m deep were carried out on Mururoa Atoll. This atoll in the Tuamotu Archipelago was also a site of nuclear testing. Ayers et al. [23] report on extensive drilling and coring on Deke Island on the Pingelap Atoll of the Eastern Caroline Islands. A review of this literature did not reveal continuous structures in Holocene sediments that are of a size comparable to the resistive features mapped by our surveying (30–200 m), however.

Shallow cores are less available on fringing reefs. Gischler et al. [36] cored two traverses consisting of three holes each on the reefs of Bora-Bora, French Polynesia. One traverse was in the fringing reef and the other in the barrier reef. Cores were collected on the barrier reef of Papeete, Tahiti, but these were all deep cores, so the shallow environment was not reported in detail. The Hanauma fringing reef of Oahu was extensively cored in a 150 m transect to a depth of about 20 m [42] and remains one of the mostly densely sampled fringing reefs [2]. Stratigraphic interpretation suggested that the reef was built upon isolated coral heads which coalesced laterally as coral and calcareous algae become more prevalent [42]. The length-scale of these laterally coalesced features was not identifiable in the transects, however.

2. Material and Methods

2.1. Study Site

Mo'orea is a high volcanic island in the Society Islands Archipelago and part of French Polynesia, an overseas collectivity of France. It is located about 16 km northwest of Tahiti, with an area of approximately 130 km^2 and a maximum elevation of 1207 m. The annual mean air temperature is 25 °C. The island has a cooler and drier winter from May to November and a warmer, wetter summer from November to April. Mo'orea receives between 2995 mm and 3245 mm of rainfall every year [43]. It is populated with about 18,000 inhabitants and has an active agricultural and tourist economy.

Mo'orea is surrounded by a fringing/barrier reef. While the eastern side of the island is dominated by barrier reefs with deep lagoons, the western side is dominated by wide (~1 km) fringing reef flats with a few sections toward the south with more prominent lagoons (Figure 1). Our study site focused on the fringing reef sections that present extensive reef flats that are traversed by narrow shore-parallel boat channels. Internal wave activity is high from October to May and markedly lower from June to September [44]. The observed tides in Mo'orea are unusually small (on the order of 0.2 m amplitude at spring tide), resulting from its location within the South Pacific amphidromic system [45].

The largest peak is at the S_2 frequency, with a smaller peak at the M_1 frequency, and a significantly smaller peak at the O_1 frequency.

Drill cores in French Polynesia indicate that coral reefs have accreted over the past 16,000 years [46]. Growth rate decreased in the Holocene and ceased when the sea level stabilized about 6 kyr BP. Both empirical data and modeling indicate that the sea level in the Society Islands has dropped by ~2 m since the Holocene maximum at ~4.5 ka BP, corresponding to a rate of about 0.4 mm/yr [47]. The subsidence rate of Mo'orea has been estimated to be 0.14 mm/yr, based on petrological analysis of the emerged reef conglomerate [48].

Unfortunately, no boreholes have penetrated the reefs of Mo'orea below about 1 m. Shallow cores of calcareous sand were taken in support of a pier construction near Haapiti [49], but these samples did not include indurated material that could potentially confine groundwater. Our cores, collected using a handheld coring drill (Shaw Portable Core Drill, Yamhill, OR, USA), generally found that near-shore fringing reefs were covered by a thin indurated carbonate layer below about 10–30 cm of lose carbonate sediment. This layer is often referred to as a reef flat plate (or papa in Polynesian) which is known to confine groundwater on atolls [25,50–52] and carbonate islands [25]. Electrical resistivity profiling at multiple near-shore locations indicated the presence of freshened water confined below the reef flat plate [10]. More recently, our coring and sampling through the reef flat plate near the Berkeley Gump Station and on the western coast of Mo'orea revealed confined brackish water. Due to leakage of the piezometer seal, the salinity was not always accurately measured but in at least one good measurement water below the reef flat plate was about half ocean salinity.
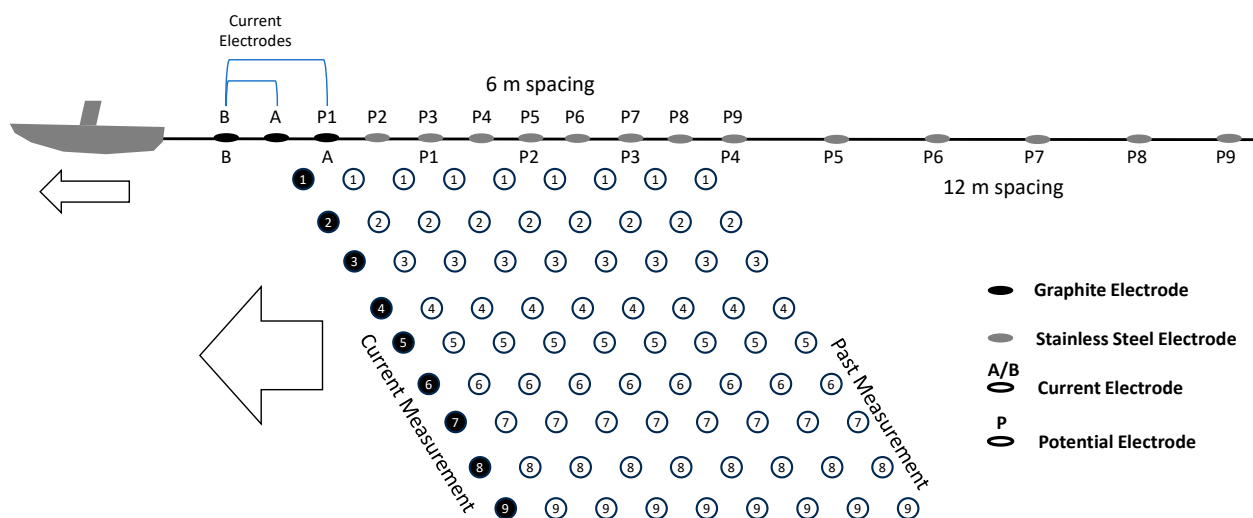
2.2. Electrical Resistivity Tomography

Electrical resistivity can provide a means by which sub-reef geologic structures can be profiled non-invasively invasively [15,53,54]. The premise is that, when an electrical current is passed through the subsurface, the measured voltage-drop will reflect a combination of the porosity of the subsurface sediments and the salinity of the subsurface fluids. Therefore, in seawater-saturated sediments, electrical resistivity profiling produces only an estimate of porosity, whereas, in homogenous aquifers, such profiles would indicate variations in groundwater salinity. Given the wide range in porosity between unconsolidated coral sediments and lithified coraline structures [15,55], electrical resistivity profiles can elucidate shallow sedimentary structures in reef flats if pores are saturated with seawater.

To obtain a subsurface bulk resistivity profile of ER, many current and electrical potential pairings (quadripoles) are used [56]. For land-based surveys, electrodes are coupled to the ground by staking or burying them, but, for water-based surveys, current is passed directly to the water column. In general terms, the greater the maximum electrode separation, the deeper the measurement of ER. Many overlapping quadripole measurements allow the generation of a composite dataset of the subsurface electrical resistivity structure. However, the potential measurements represent an integration of electrical current loss along the entire electron pathway, so measurement of ER at a single location must be obtained through inversion of many quadripole measurements (i.e., tomography). Inversion is accomplished by generating realizations (models) of the subsurface ER structure and using an optimization algorithm to find the best fit to the measured voltage loss at the electrodes [56]. The extraction of an ER profile from measured data is, therefore, non-unique and somewhat spatially ambiguous. When ER profiles are collected in marine environments, much of the current is taken by the highly conductive seawater column. This "current channeling" leads to a severe degradation of the quality of subsurface ER profiles [54]; a problem highlighted by the data collected in this study.

2.3. Boat-Towed Continuous Electrical Resistivity Profiling (CRP)

ER profiles can be collected using a boat-towed electrode array to profile sub-bottom ER structure in freshwater and marine environments [54]. Electrode arrays that collect data while moving have more limited options with respect to measurement strategies than static arrays. Figure 1 illustrates data collection for a boat-towed CRP survey for an eight-channel resistivity system after [54]. In this example, the first two electrodes on the streamer are used to inject current and the remaining nine nodes are used to measure electrical potential. As the potential is measured farther from the current pair, resistivity is measured at greater depth. This is illustrated by the pseudosection shown schematically in Figure 2: Electrode layout for boat-towed CRP survey showing the 6 m and 12 m spacing options to vary measurement depth. Resistivity measurements are organized in a "pseudosection" illustrated by the numbered circles. One diagonal of data is collected at each acquisition time. These measurements cannot be repeated as the boat is moving continuously. For our system, an Advance Geosciences Incorporated (AGI, Austin, TX, USA) 8-channel, 200-watt system, the streamer nodes are constructed of stainless steel and graphite. Graphite is used for current injection to prevent corrosion in seawater. Boat speeds are kept to below about 4 knots (7.4 km/h) to allow time for acquisition. Even at these slow boat speeds, however, 10 s of kilometers of data can be collected in a single day. A GPS system and depth transducer are linked to the system via a wireless connection so that the profile can be geolocated while accounting for the thickness of the water column. The datafiles collected during the survey are ingested into the software EarthImager 2D® to perform the inversion and create a continuous profile.

Figure 2. Electrode layout for boat-towed CRP survey showing the 6 m and 12 m spacing options to vary measurement depth. Resistivity measurements are organized in a "pseudosection" illustrated by the numbered circles. One diagonal array of data is collected at each acquisition time. These measurements cannot be repeated as the boat is moving continuously in the direction indicated by the arrows.

For the marine CRP system we used, the depth of ER acquisition can be adjusted by changing the configuration of the current and potential nodes. Figure 2 illustrates the configuration available for 6 m and 12 m configurations. We initially used the shallower 6 m configuration to enhance shallow ER data density. However, we found that the 15 m deep profiles produced from this configuration made it difficult to distinguish reef structures, so we moved to the 12 m configuration, which produces an ER profile about 30 m deep. Note that on the reef flat, boat movement was limited to dredged boat channels. Coral pinnacles made movement impractical outside of the boat channel in most areas of the fringing reef. The towed array in the 12 m configuration is about 170 m long, so maneuverability is limited.

2.4. Inversion of ER Tomography Data

Electrical resistivity data must be inverted to obtain a gridded profile of ER estimates [56,57]. Optimization algorithms are used to find a subsurface distribution of ER that could have produced the measurements collected. The general procedure is to generate multiple forward simulations of ER data collection, each of which has a different ER structure, and compare the simulated measurements to the actual measurements. The misfit between simulated and actual ER measurements is reduced through an optimization algorithm. There are various software packages available for performing ER tomography inversion [57] but we used the software designed for our acquisition system, EarthImager 2D® [58].

The inversion process is over-parameterized, meaning there are many more ER data points in the profile than there are measurements. To create a mathematically stable solution, a technique called regularization must be used. In regularization, the solution increases the smoothness of the resulting profile under the assumption that an ER grid value is likely to be next to a similar ER grid value. The parameters used for regularization can have a marked effect on the profile heterogeneity. Too much regularization (i.e., over-smoothing) may lead to a loss in spatial resolution, but too little regularization (i.e., over-fitting) can lead to inversion of noise in the dataset [56]. Consequently, some expectation of the subsurface ER structure should guide the inversion parameters used.

Another important consideration for inversion is the matching of the ER targets to the survey design. For example, targets smaller than the node-spacing cannot be confidently resolved. In marine surveys, electrical current channeling in the water column can lead to a severe degradation in the ability to invert resistive features [15,54]. This is a particular problem in CRP surveys because they cannot use data-stacking to reduce errors. In our case, because we were interested in resolving lateral heterogeneities in sub-bottom ER, we performed forward simulations of CRP profiles of generic targets to constrain confidence in the inversion process (Section 4.1).

2.5. Archie's Law

As noted previously, apparent electrical resistivity derived from ER tomography is related to geologic parameters of interest through Archie's Law:
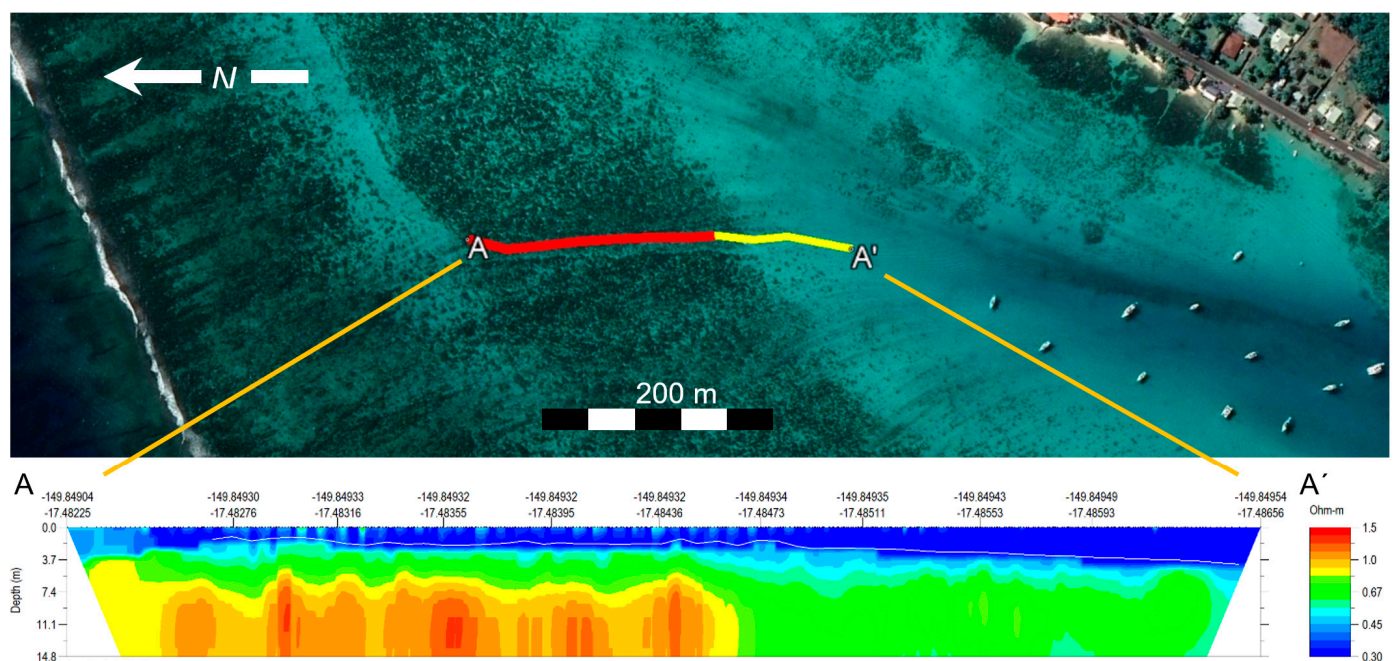
$$\rho_b = \rho_f n^{-m} \tag{1}$$

where ρ_b is the measured bulk resistivity (usually measured in ohm-m), ρ_f is the pore-fluid resistivity, n is the porosity, and m is a "cementation factor" which accounts for the tortuosity of the pore pathways as experienced by moving electrons [57]. Archie's Law requires that two parameters be specified, so that a third can be related to the measured bulk resistivity. Of the three parameters related to measured bulk resistivity, m, is the most difficult to estimate. In practice, the cementation factor can be measured only in the laboratory samples where the other parameters can be measured independently. Experiments suggest that m should be about 1.5 to 2.0 for unconsolidated marine sands [59] and close to 2.0 for cemented oil reservoir rocks [55]. The m value is expected to increase from 2 to 5 with increasing porosity in vuggy carbonate rocks [55].

Some authors have observed resistive anomalies on reef flats surrounding carbonate islands and attributed them to confined freshened water [10,15,16]. Such a determination of freshened porewater is difficult to make with confidence, given the confounding effects of porosity and the cementation factor (Equation (1)). Importantly, substrata on reef flats are expected to be composed of loose carbonate detritus or sand, lithified coral structures, and cemented carbonate material. Strata can, consequently, have a wide range of porosity and cementation factor, which can affect measured bulk resistivity, ρ_b, even when pore-fluid resistivity is constant. Subsurface resistive anomalies measured using ER tomography may be interpreted with respect to contrasts in porosity or pore fluid salinity.

However, the indication that either porosity or pore-fluid salinity varies in reef structure suggests spatial heterogeneity in the diagenesis of reef carbonates and possibly the migration of groundwater confined within the reef. The two processes are potentially interrelated, with groundwater carrying carbonic acid that leads to dissolution and recementation of carbonate [60]. In this work, we do not attempt to quantify porosity or fluid resistivity from the CRP profiles we collected. Other researchers have attempted to make these determinations [15], but, based upon our forward modeling, we do not believe such a determination is justified in the absence of direct sampling of either porosity or fluid resistivity.
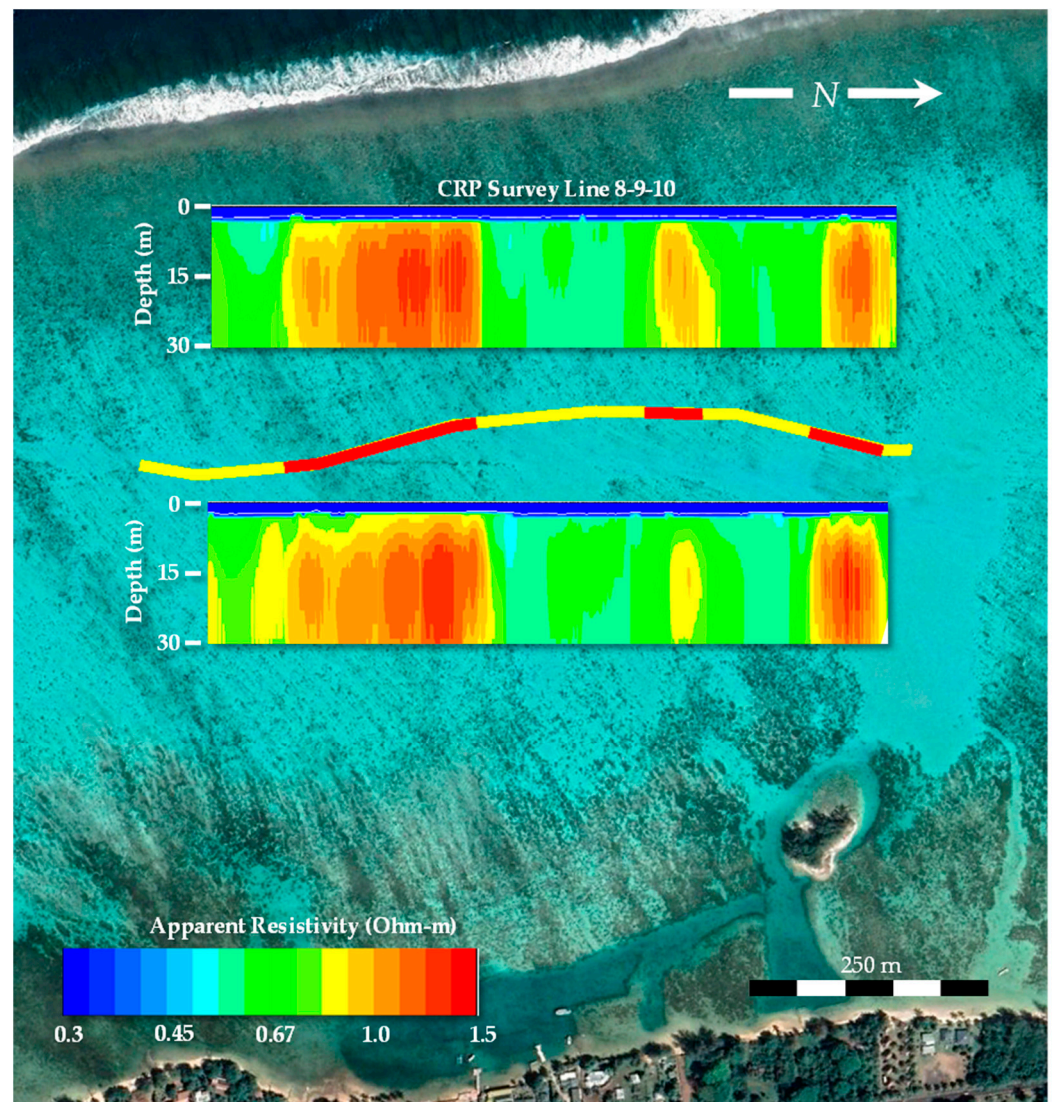
3. Results

The boat-towed CRP ER survey lines are summarized in Figure 1. The survey line on the north side of the island was a 6 m array, with a profile depth of about 15 m, while all others were collected using a 12 m array, with a profile depth of 30 m (Figure 2). All surveys results are presented in the Supplemental Material. Representative surveys are discussed here. Figure 3 shows example results from a CRP survey in which a 6 m nodal spacing was used. The mapped survey course is shown in the upper satellite image (yellow line) and the inverted CRP in the lower figure. The depth of the sea bottom, measured by the GPS-tagged sonar depth ranger, is shown as a white line. Seawater resistivity was not specified in the inversion but was optimized to 0.25 ohm-m during the inversion process, which is similar to the expected seawater resistivity of 0.27 ohm-m computed from measured salinity. The inverted bulk ER over the reach dominated by coral heads exceeds that of the loose lagoon sediments by about a factor of two. ER varies within the coral dominated reach as well, ranging from about 0.9 to 1.5 ohm-m. Our forward modeling (Section 4.1) suggests that the inverted resistivity values are not quantitatively accurate, i.e., the magnitudes are likely incorrect, but the fine-scale heterogeneity of ER is qualitatively correct.

Figure 3. CRP profile with 6 m node spacing over coral reef and lagoon sediments. Resistive features are indicated in the survey course in red.
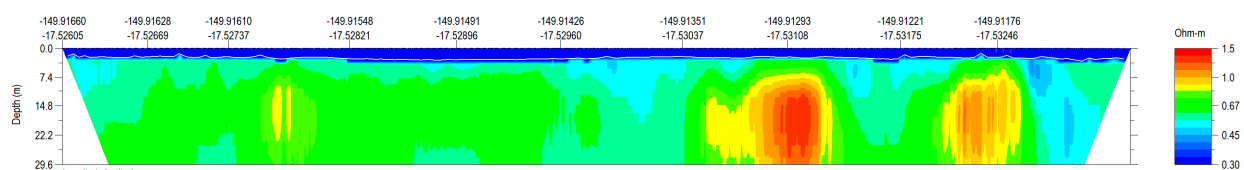
Figure 4 shows repeated CRP surveys in which a 12 m nodal spacing was used. The imaging depth is about twice that of the previous profile with a 12 m nodal spacing. The profiles were collected in two different boat directions, north–south in the upper and south–north in the lower profile. Resistive features are apparent in both profiles and these features

are repeatable. This provides some confidence in the imaging method. The full path is shown in yellow and the ER features are highlighted in red in the satellite image.
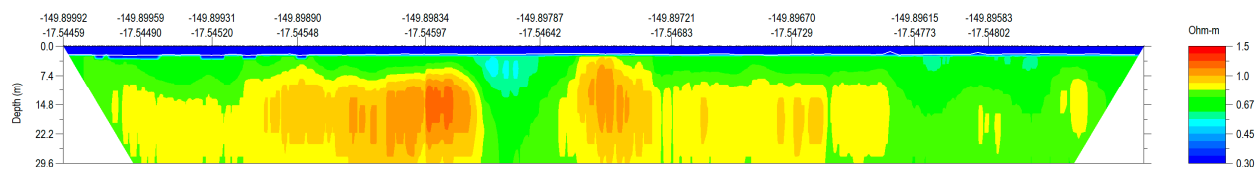

Figure 4. CRP survey repeated section. Resistive anomalies shown on the ER profiles are highlighted in red on the survey course.

Figures 5 and 6 show two more representative profiles (see Supplemental Material for mapped locations). Figure 5 is typical of profiles that showed distinct isolated features, with an apparent bulk resistivity about 300% of background. Figure 6 shows more diffuse features with an apparent bulk resistance only about 150% of background. See Supplemental Material for a presentation of all profiles.

Figure 5. CRP Survey 5-26-4 showing isolated resistive features (see Supplemental Material for map location).

Figure 6. CRP Survey 8-9-3 showing more continuous resistive features (see Supplemental Material for map location).
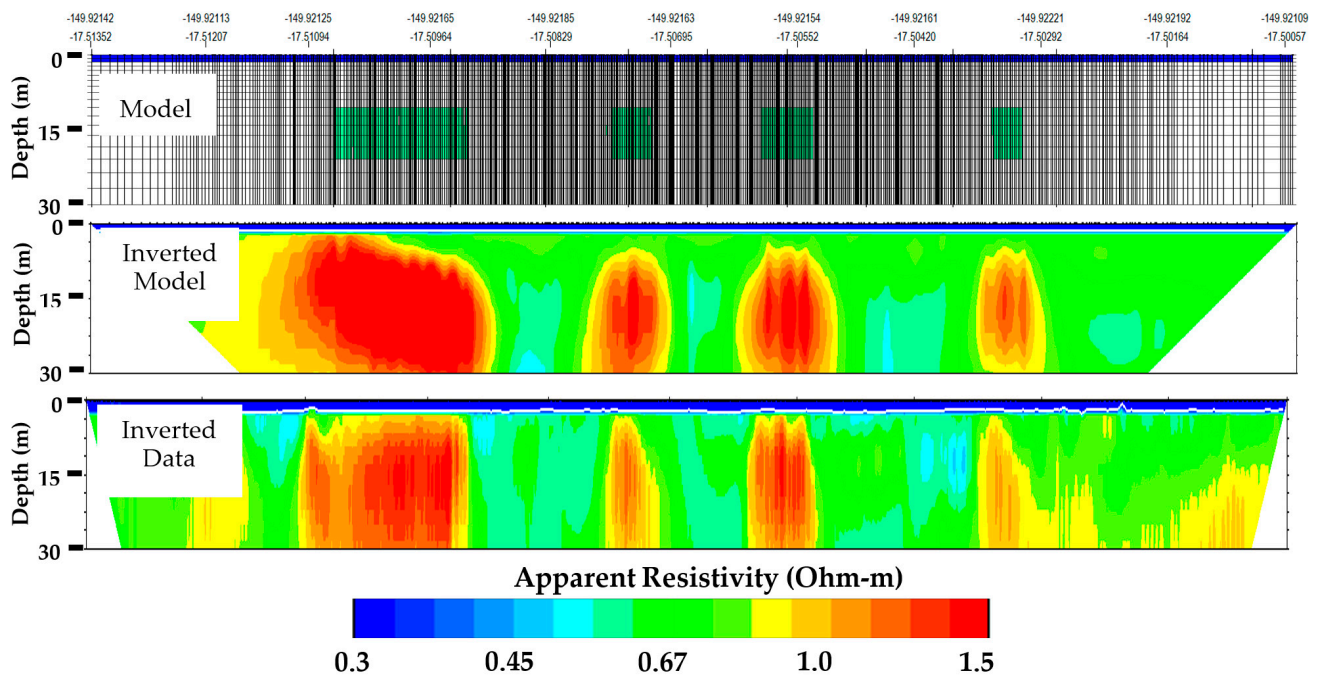
4. Discussion

As noted, CRP imaging in marine environments is limited by current channeling in seawater and the lack of repeated measurements due to the constantly moving electrodes. Consequently, we begin our discussion of results with some synthetic modeling to assess the resolution of the imaging technique.

4.1. ERT Sensitivity to Resistivity Anomalies

Resolution of an ER target through the inversion process is affected by the contrast in ER, the size of the target, and the depth of the target. The ability to resolve larger targets must be assessed through forward modeling. In forward modeling, synthetic resistivity measurements are generated using a numerical representation of an ER structure in a numerical grid. These synthetic measurements are then inverted using the same method used to invert real data. In this manner, the ability of the inversion process to resolve ER anomalies and structures can be assessed, relative to actual survey designs and inversion parameters.

Befus et al. [15] performed forward modeling for their boat-towed CRP profiles conducted on the fringing reef of Rarotonga, Cook Islands, an environment very similar to Mo'orea. Forward modeling indicated that highly resistive features could not be properly resolved in either static or CRP profiles, due primarily to current channeling in the marine water column. For example, a 500 Ω-m target in a 0.431 Ω-m background was inverted to have an ER of 8.1 Ω-m in CRP surveys. Day-Lewis et al. [54] performed generic forward modeling to evaluate the effect of marine current channeling in "blunting" the inverted resistivity of a target. They found that a 2 Ω-m target in a 1.3 Ω-m background was inverted as 1.6 Ω-m, while a 200 Ω-m target inverted as 2.7 Ω-m. The larger the contrast in ER between the target and the background, the more extreme the underestimation of the target during inversion.

We created synthetic models to assess the ability of ER CRP surveys to identify ER heterogeneities in the reef flat. In this trial-and-error exercise, an attempt was made to approximately replicate the profile 8-9-10. The process begins with hypothesizing a numerical resistivity model (Figure 7, top). Our model consisted of three isolated resistive features that extended between 10 and 20 m below sea level and were assumed to have an ER of 10 Ω-m, considered to be an upper limit of bulk resistivity for vuggy carbonates as reported by Jackson [59,61]. The background was assumed to have an ER of 0.5 Ω-m (typical for our measured profiles) and seawater 0.27 Ω-m (based upon ocean water salinity). The model grid reflects the actual distribution of measurements collected from a profile (5-26-1) to provide a realistic density of grid spacing. The ER measurements that would be collected using this measurement density are simulated in forward finite element modeling to produce an array of apparent bulk resistivity measurements called a pseudosection (see Figure 2). This pseudosection is then inverted using the same parameters used for inversion of actual measured pseudosections to create a synthetic inverted resistivity profile.

Figure 7. A synthetic model of 10 ohm-m ER anomalies measured using the actual boat-towed CRP quadripole measurements (**top**), the inversion of those simulated ER measurements (**middle**) compared with the actual inverted survey from survey 8-9-10 (**bottom**).

Comparison of the "true" model resistive features (Figure 7, top) and the inverted synthetic profile (Figure 7, middle) illustrate the loss of detailed geometry that is characteristic of ER surveys. Better resolution of geometry can be obtained in static surveys where multiple quadripoles at a varying separation measure the same point in the subsurface. Repeated measurements particularly improve the vertical resolution of the profile. Reciprocal measurements (i.e., duplicate measurements with reversed voltage polarity) also improve the accuracy of the ER measurements. Repeat and reciprocal measurements are not possible in CRP surveys because the array is constantly moving. Combined with the aforementioned blunting because of current loss in the seawater column, this results in limited resolution of subsurface resistive features.

However, the synthetic and actual inverted sections are qualitatively similar. Through systematic variation in the geometry of the resistive features, some constraint could be placed on the inverted actual profiles. We systematically varied the width and depth of the three features and compared the inverted synthetic and real profiles. The low resistivity-gap between seawater and the resistive features could not be replicated with targets shallower than 10 m, but features with an upper limit as deep as 15 m produced reasonable approximations of the inverted profile. Similarly, systematically varying the thickness of the targets suggests that there must be a lower limit to the resistive feature. The decreasing resistivity of the targets near the bottom of the profile could not be represented with features that extended deeper than about 20 m. Wider resistive targets resulted in a loss of distinctly separate features, as seen in the actual inverted profile. Although changing the regularization parameters in the inversion algorithm produced variations in level of detail in the resistivity profile, all tested parameters produced distinctly identifiable resistive features at depth. The magnitude of the inverted feature was not accurately inverted, however. The true (synthetic) resistivity of the features of 10 Ω-m was inverted to be about 1.7 Ω-m. In practice, true (synthetic) resistivity features with the same geometry but magnitudes at 100 Ω-m and larger produced similar inverted profiles.

4.2. Interpretation of the CRP Profiles

Our synthetic sensitivity modeling indicates that the resistive structures imaged by the CRP surveys are real and repeatable, but the depths and extents are approximate, and the magnitude of ER is largely undetermined. Archie's Law suggests that we are looking for features with smaller porosity and/or freshened water to account for the increase in ER. Direct sampling through coring and fluid-sampling would be necessary to ascertain the nature of the structures, and this has yet to be accomplished on the reefs of Mo'orea. The question then is: what can be learned about reef structure with the limited ER information available?

4.2.1. Resistive Heterogeneity Explained by Porosity Variation

If we assume that all pores are saturated with pure seawater, then we must hypothesize reef structures with reduced porosity that could produce anomalously resistive features as imaged by CRP. These features were imaged to be about 10–20 m deep and range in width between about 30–200 m measured parallel to shore. The modern geomorphic features that dominate the reef flat are coral heads, coral clusters, and microatolls [20]. None of these individual features are greater than 30 m in size, but coral does tend to cluster and form geomorphic striations in sizes within this range (e.g., Figure 4). ER anomalies imaged at depth do not correspond with surface expressions of coral, but deep features could represent coral communities and clusters that have lithified to produce low-porosity ER anomalies. The sedimentological model for this is not apparent. It has been suggested that one reef-building mechanism is the infilling of coral heads by coraline algae [42]. This may result in a patchy cementing of reefs.

The profiles are difficult to explain with normal reef-construction processes. Reef buildup should occur continuously, so that there would be many such anomalies overlapping through the profile at various depths, unlike the distinct features with uniform depth imaged by CRP. Current channels that formed during lower sea-stands may have created opportunities for variable cementation. Another potential explanation is that these anomalies are rip-up deposits from a very large storm or tsunami. Blocks of carbonate from outer reef edges thrown onto reef flats can be 20 m long [20,41]. However, we observed similar anomalies on both the northern and western reef flats of Mo'orea and it seems unlikely that a storm or tsunami would deposit blocks on both sides. In addition, some features are too large (~200 m) to be rip-up deposits. This hypothesis does not seem supported by our surveys.

A more attractive explanation is that the resistive features are associated with a lower sea-stand, especially the top of the Pleistocene reef deposits. Pleistocene deposits were exposed to air during low sea-stands and are, therefore, generally well-cemented and in some cases dissected by dissolution to form karst features [2]. The thickness of Holocene deposits is expected to be highly variable among islands and even within islands. Gischler et al. [62] used seismic surveys and coring to measure Holocene lagoon deposits over Pleistocene units that were 10–12 m thick, while barrier reef Holocene sediments over Pleistocene units were 30 m thick. Coring on Tahiti Barrier reefs showed Holocene sequences of >87 m thickness overlying Pleistocene limestone [63]. Gischler et al. [36] summarize sea-level data from their own work and others for the Society Islands and found relative sea levels to be 10 m lower at about 6–8.6 kya. Rashid [47] examined relative sea level on Mo'orea, but did not estimate levels prior to the Holocene when relative sea level was more than 10 m below present levels. Consequently, the depth to the Holocene/Pleistocene boundary on the reef flats of Mo'orea could potentially be 10–15 m deep, but it is undetermined based upon available information.

We investigated the hypothesis that the resistive features could be rough topography formed through karstification during sub-aerial exposure of Pleistocene reefs. Uplifted Pleistocene limestone on South Pacific islands do show a very rough topography, sometimes dominated by pinnacles of resistant limestone [20]. Rough topography from paleokarst has been imaged in high-resolution seafloor and seismic surveys [36,38]. Shallow seismic

mapping of the Great Bahama Bank showed a complex Pleistocene topography that included sinkholes and channels with depths ranging from 4 to 18 m below the modern reef surface [64]. We attempted to produce individual resistive features by simulating a base of resistive material near the bottom of the profile with protruding pinnacles of resistive rock reaching 5–10 m high. Even with such unrealistically large pinnacle heights, the individually distinct resistive features in the inverted profiles could not be produced. Our CRP profiles, consequently, are not consistent with, but do not rule out an explanation of, karst surface topography.

4.2.2. Resistive Heterogeneity Explained by Porewater Salinity

It is intriguing to hypothesize that a Pleistocene karstic system confines freshened water, which was imaged by our surveys. The upper Pleistocene is well-known to transmit freshened water on atolls [23,25,27,65]. The contact between the Holocene and Pleistocene is called the Thurber discontinuity in reference to aquifers, because the permeability of the Pleistocene strata can be an order of magnitude greater than the overlying Holocene units [27]. Although this has been documented on atoll islets (motu), it has yet to be shown in fringing or barrier reefs.

Befus et al. [15] conducted CRP surveys using the same instrument as our own on the fringing reef of Rarotonga, Cook Islands. Their CRP profiles look strikingly like our own, with isolated resistive features apparent in most. Their interpretation, based upon forward modeling and Archie's Law, is that these features could be related to freshened water confined in consolidated reef carbonates. Interpretation of Archie's Law was based upon forward modeling that suggested, like our models, that current channeling vastly blunts the ER signal. They conjectured that the true ER of these features was much greater than the 3–5 ohm-m resistance inverted from their surveys, adding weight to the interpretation that freshened water caused the imaged ER anomalies. Tait et al. [16] had previously shown that, in one CRP profile, an isolated resistive feature could be correlated to a small drop in seawater temperature at the same location. The isotope ^{222}Rn, which is often used as a tracer of groundwater, was also elevated at this general position in the reef. Several lines of evidence, therefore, suggest the presence of confined groundwater in a fringing reef environment similar to that of Mo'orea.

Our own near-shore static marine ER surveys [10], combined with recent coring and water-sampling, have shown that resistive fresh water can be trapped below the near-shore western fringing reef of Mo'orea. However, this water is trapped just below the sea bottom and does not indicate that freshened water is confined within deeper carbonate units like Pleistocene karst. Given the prevalence of the Thurber discontinuity documented on atolls, it is not unreasonable to conjecture that deep water recharged in the volcanics of Mo'orea try to exit within the fringing reef and become trapped at least partially below Holocene sediments. Karst conduits or associated conduits of 20–200 m in width are consistent with exposed karst observed in uplifted pacific island carbonate terrains [20].

5. Conclusions

Boat-towed continuous resistivity profile (CRP) surveys were conducted along the fringing reefs of the high-island of Mo'orea, French Polynesia. These surveys identified localized resistive features that extended about 10–20 m below sea level and a width, parallel to shore, of 20–300 m, and had an apparent bulk resistivity 1.5 to 3 times that of the surrounding material. According to Archie's Law, an increase in electrical resistivity can be explained either by a reduction in porosity or porewater-salinity relative to background. As reported by others, CRP profiles collected in marine environments are difficult to interpret quantitatively due to the lack of repeat measurements and the loss of current to the highly conductive seawater column. Without coring through the reef, we cannot decouple the effects of porosity and salinity in the interpretation of these profiles.

We are unable to hypothesize a scenario in which cementation would occur at a fairly uniform depth of about 10 m below sea level (or 8 m below the sea floor). A more likely

explanation is that freshened water is confined below the reef. Similar resistive features measured by others using CRP on the fringing reef of Rarotonga [15,16] support this interpretation. Static ER profiles collected by our team on Mo'orea have shown near-shore resistive layers in the reef that appear to be confined groundwater [10]. However, the confining unit in this case is a thin "reef flat plate" composed of lithified sediments just below the sea floor, so it is not consistent with the deeper features identified in CRP surveys. Groundwater is known to be confined within Pleistocene limestone below lower-permeability Holocene sediments on atolls. The same contact may explain confined groundwater in the fringing reef of Mo'orea, but this is conjecture. The depth of the Pleistocene/Holocene contact on the reef of Mo'orea is not known, but, based upon cores collected on Bora Bora, could reasonably occur at the 10 m depth where the resistive features are found.

Although CRP surveys are an attractive tool for identifying freshened water in reefs, they are not as reliable as early studies have indicated. Multiple researchers have identified problems with current loss in the seawater column that results in a blunting of the resistivity measurements. Above a certain threshold, a resistance contrast between a target and background cannot be quantified. As a result, the effects of porosity and fluid-salinity on apparent resistivity cannot be separated. The primary usefulness of CRP surveys, in our estimation, is to identify potential targets for invasive sampling. We are currently planning coring and water-sampling based upon the surveys reported here.

The potential for sub-reef groundwater movement has important implications for the understanding, protection, and management of reefs surrounding high tropical islands. High islands have substantial runoff that brings nutrients or pollution to the reef ecosystem depending on island land-use. Characterizing the distribution of runoff to the shoreline, through the reef, or under the reef, is a fundamental step in understanding the complex interconnection between these fragile terrestrial and marine ecosystems.

References

1. Starke, C.; Ekau, W.; Moosdorf, N. Enhanced Productivity and Fish Abundance at a Submarine Spring in a Coastal Lagoon on Tahiti, French Polynesia. *Front. Mar. Sci.* **2020**, *6*, 809. [CrossRef]
2. Kennedy, D.; Woodroffe, C. Fringing reef growth and morphology: A review. *Earth-Sci. Rev.* **2002**, *57*, 255–277. [CrossRef]
3. Carlson, R.R.; Foo, S.A.; Asner, G.P. Land Use Impacts on Coral Reef Health: A Ridge-to-Reef Perspective. *Front. Mar. Sci.* **2019**, *6*, 562. [CrossRef]

4. Bishop, J.M.; Glenn, C.R.; Amato, D.W.; Dulai, H. Effect of land use and groundwater flow path on submarine groundwater discharge nutrient flux. *J. Hydrol. Reg. Stud.* **2017**, *11*, 194–218. [CrossRef]

5. Moosdorf, N.; Oehler, T. Societal use of fresh submarine groundwater discharge: An overlooked water resource. *Earth-Sci. Rev.* **2017**, *171*, 338–348. [CrossRef]

6. Johnson, A.G.; Glenn, C.R.; Burnett, W.C.; Peterson, R.N.; Lucey, P.G. Aerial infrared imaging reveals large nutrient-rich groundwater inputs to the ocean. *Geophys. Res. Lett.* **2008**, *35*. [CrossRef]

7. Oehler, T.; Bakti, H.; Lubis, R.F.; Purwoarminta, A.; Delinom, R.; Moosdorf, N. Nutrient dynamics in submarine groundwater discharge through a coral reef (western Lombok, Indonesia). *Limnol. Oceanogr.* **2019**, *64*, 2646–122661. [CrossRef]

8. Brosnan, T.; Becker, M.W.; Lipo, C. Coastal groundwater discharge and the ancient inhabitants of Rapa Nui (Easter Island), Chile. *Hydrogeol. J.* **2018**, *27*, 519–534. [CrossRef]

9. Knee, K.L.; Crook, E.D.; Hench, J.L.; Leichter, J.J.; Paytan, A. Assessment of Submarine Groundwater Discharge (SGD) as a Source of Dissolved Radium and Nutrients to Moorea (French Polynesia) Coastal Waters. *Estuaries Coasts* **2016**, *39*, 1651–1668. [CrossRef]

10. Hagedorn, B.; Becker, M.W.; Silbiger, N.J. Evidence of freshened groundwater below a tropical fringing reef. *Hydrogeol. J.* **2020**, *28*, 2501–2517. [CrossRef]

11. Street, J.H.; Knee, K.L.; Grossman, E.E.; Paytan, A. Submarine groundwater discharge and nutrient addition to the coastal zone and coral reefs of leeward Hawai'i. *Mar. Chem.* **2008**, *109*, 355–376. [CrossRef]

12. Oehler, T.; Tamborski, J.; Rahman, S.; Moosdorf, N.; Ahrens, J.; Mori, C.; Neuholz, R.; Schnetger, B.; Beck, M. DSi as a Tracer for Submarine Groundwater Discharge. *Front. Mar. Sci.* **2019**, *6*, 563. [CrossRef]

13. Nelson, C.E.; Donahue, M.J.; Dulaiova, H.; Goldberg, S.J.; La Valle, F.F.; Lubarsky, K.; Miyano, J.; Richardson, C.; Silbiger, N.J.; Thomas, F.I. Fluorescent dissolved organic matter as a multivariate biogeochemical tracer of submarine groundwater discharge in coral reef ecosystems. *Mar. Chem.* **2015**, *177*, 232–243. [CrossRef]

14. DiNapoli, R.J.; Lipo, C.P.; de Smet, T.S.; Hunt, T.L. Thermal Imaging Shows Submarine Groundwater Discharge Plumes Associated with Ancient Settlements on Rapa Nui (Easter Island, Chile). *Remote Sens.* **2021**, *13*, 2531. [CrossRef]

15. Befus, K.M.; Cardenas, M.B.; Tait, D.R.; Erler, D.V. Geoelectrical signals of geologic and hydrologic processes in a fringing reef lagoon setting. *J. Hydrol.* **2014**, *517*, 508–520. [CrossRef]

16. Tait, D.R.; Santos, I.R.; Erler, D.V.; Befus, K.M.; Cardenas, M.B.; Eyre, B.D. Estimating submarine groundwater discharge in a South Pacific coral reef lagoon using different radioisotope and geophysical approaches. *Mar. Chem.* **2013**, *156*, 49–60. [CrossRef]

17. Mylroie, J.E.; Carew, J.L. Karst Development on Carbonate Islands. In *Unconformities and Porosity in Carbonate Strata*; Budd, D.A., Saller, A.H., Harris, P.M., Eds.; American Association of Petroleum Geologists: Tulsa, OK, USA, 1995; Volume 63. [CrossRef]

18. Halliday, W.R. History and status of the Moiliili Karst, Hawaii. *J. Cave Karst Stud.* **1998**, *60*, 141–145.

19. Darwin, C. *The Structure and Distribution of Coral Reefs*; Smith, Elder & Co.: London, UK, 1842; Volume 12, p. 3.

20. Guilcher, A. *Coral Reef Geomorphology*; John Wiley & Sons: New York, NY, USA, 1988.

21. Ladd, H.S.; Schlanger, S.O. *Drilling operations on Eniwetok Atoll, Bikini and Nearby Atolls, Marshall Islands*; United States Geological Survey Professional Paper: Reston, VA, USA, 1960; 260-Y; pp. 863–903.

22. Quinn, T.M.; Saller, A.H. Chapter 21—Geology of Anewetak Atoll, Republic of the Marshall Islands. In *Developments in Sedimentology*; Vacher, H.L., Quinn, T.M., Eds.; Elsevier: Amsterdam, The Netherlands, 2004; Volume 54, pp. 637–666.

23. Ayers, J.F.; Vacher, H.; Clayshulte, R.N.; Strout, D.; Stebnisky, R. *Hydrogeology of Deke Island, Pingelap Atoll, Eastern Caroline Islands*; School of Geosciences Faculty and Staff Publications: Tampa, FL, USA, 1984.

24. Vacher, H.L.; Ayers, J.F. Hydrology of small oceanic islands—Utility of an estimate of recharge inferred from the chloride concentration of the freshwater lenses. *J. Hydrol.* **1980**, *45*, 21–37. [CrossRef]

25. Bailey, R.T.; Jenson, J.W.; Olsen, A.E. Estimating the Ground Water Resources of Atoll Islands. *Water* **2010**, *2*, 1–27. [CrossRef]

26. Werner, A.D.; Sharp, H.K.; Galvis, S.C.; Post, V.E.; Sinclair, P. Hydrogeology and management of freshwater lenses on atoll islands: Review of current knowledge and research needs. *J. Hydrol.* **2017**, *551*, 819–844. [CrossRef]

27. Buddemeier, R.W.; Oberdorfer, J.A. *Hydrogeology and Hydrodynamics of Coral Reef Pore Waters*; 6. International Coral Reef Symposium, No. UCRL-98872; CONF-880873-2, Townsville; Lawrence Livermore National Lab.: Livermore, CA, USA, 1988.

28. Oberdorfer, J.A.; Buddemeier, R.W. Coral-reef hydrology: Field studies of water movement within a barrier reef. *Coral Reefs* **1986**, *5*, 7–12. [CrossRef]

29. Mylroie, J.E.; Jenson, J.W.; Taborosi, D.; Jocson, J.M.; Vann, D.T.; Wexel, C. Karst features of Guam in terms of a general model of carbonate island karst. *J. Cave Karst Stud.* **2001**, *63*, 9–22.

30. Parra, S.M.; Valle-Levinson, A.; Mariño-Tapia, I.; Enriquez, C. Salt intrusion at a submarine spring in a fringing reef lagoon. *J. Geophys. Res. Ocean.* **2015**, *120*, 2736–2750. [CrossRef]

31. Houben, G.J.; Stoeckl, L.; Mariner, K.E.; Choudhury, A.S. The influence of heterogeneity on coastal groundwater flow—Physical and numerical modeling of fringing reefs, dykes and structured conductivity fields. *Adv. Water Resour.* **2018**, *113*, 155–166. [CrossRef]

32. Cardenas, M.B.; Zamora, P.B.; Siringan, F.P.; Lapus, M.R.; Rodolfo, R.S.; Jacinto, G.S.; Diego-McGlone, M.L.S.; Villanoy, C.L.; Cabrera, O.; Senal, M.I. Linking regional sources and pathways for submarine groundwater discharge at a reef by electrical resistivity tomography, ^{222}Rn, and salinity measurements. *Geophys. Res. Lett.* **2010**, *37*. [CrossRef]

33. Silbiger, N.J.; Donahue, M.J.; Lubarsky, K. Submarine groundwater discharge alters coral reef ecosystem metabolism. *Proc. R. Soc. B Biol. Sci.* **2020**, *287*, 20202743. [CrossRef]

34. Rougerie, F.; Fichez, R.; Dejardin, P. Geomorphology and Hydrogeology of Selected Islands of French Polynesia: Tikehau (Atoll) and Tahiti (Barrier Reef). In *Geology and Hydrogeology of Carbonate Islands. Developments in Sedimentology*; Vacher, H.L., Quinn, T.M., Eds.; Elsevier: Amsterdam, The Netherlands, 2004; pp. 475–502.

35. Orme, G.; Flood, P.G.; Sargent, G. Sedimentation trends in the lee of outer (ribbon) reefs, northern region of the Great Barrier Reef province. *Philos. Trans. R. Soc. Lond. Ser. A Math. Phys. Sci.* **1978**, *291*, 85–99.

36. Gischler, E.; Hudson, J.H.; Humblet, M.; Braga, J.C.; Eisenhauer, A.; Isaack, A.; Anselmetti, F.S.; Camoin, G.F. Late Quaternary barrier and fringing reef development of Bora Bora (Society Islands, south Pacific): First subsurface data from the Darwin-type barrier-reef system. *Sedimentology* **2016**, *63*, 1522–1549. [CrossRef]

37. Toomey, M.R.; Woodruff, J.D.; Donnelly, J.P.; Ashton, A.D.; Perron, J.T. Seismic evidence of glacial-age river incision into the Tahaa barrier reef, French Polynesia. *Mar. Geol.* **2016**, *380*, 284–289. [CrossRef]

38. Grigg, R.; Grossman, E.; Earle, S.; Gittings, S.; Lott, D.; McDonough, J. Drowned reefs and antecedent karst topography, Au'au Channel, S.E. Hawaiian Islands. *Coral Reefs* **2002**, *21*, 73–82. [CrossRef]

39. Woodroffe, C.D. *Coasts: Form, Process and Evolution*; Cambridge University Press: Cambridge, UK, 2002.

40. Bailey, R.T.; Jenson, J.W.; Rubinstein, D.; Olsen, A.E. *Groundwater Resources of Atoll islands: Observations, Modelling and Management: Technical Report 119*; Water and Environmental Research Institute of the Western Pacific, University of Guam: Mangilao, Guam, 2008.

41. Chevalier, J.; Denizot, M.; Mougin, J.; Plessis, Y.; Salvat, B. *Etude Géomorphologique de l'Atoll de Mururoa (Tuamotu)*; Cah Pac, 12, 1-144; Royal Society of London: London, UK, 1969.

42. Easton, W.; Olson, E. Radiocarbon profile of Hanauma Reef, Oahu, Hawaii. *Geol. Soc. Am. Bull.* **1976**, *87*, 711–719. [CrossRef]

43. Laurent, V.; Maamaatuaiahutapu, K.; Brodien, I.; Lombardo, S.; Tardy, M.; Varney, P. *Atlas Climatologique de la Polynésie Française*; Météo France, Délégation Interrégionale de Polynésie Française: Faa'a, Tahiti, French Polynesia, 2019.

44. Leichter, J.J.; Stokes, M.D.; Hench, J.L.; Witting, J.; Washburn, L. The island-scale internal wave climate of Moorea, French Polynesia. *J. Geophys. Res. Ocean.* **2012**, *117*. [CrossRef]

45. Hench, J.L.; Leichter, J.J.; Monismith, S.G. Episodic circulation and exchange in a wave-driven coral reef and lagoon system. *Limnol. Oceanogr.* **2008**, *53*, 2681–2694. [CrossRef]

46. Hallmann, N.; Camoin, G.; Eisenhauer, A.; Samankassou, E.; Vella, C.; Botella, A.; Milne, G.; Pothin, V.; Dussouillez, P.; Fleury, J.; et al. Reef response to sea-level and environmental changes in the Central South Pacific over the past 6000 years. *Glob. Planet. Chang.* **2020**, *195*, 103357. [CrossRef]

47. Rashid, R.; Eisenhauer, A.; Stocchi, P.; Liebetrau, V.; Fietzke, J.; Rüggeberg, A.; Dullo, W.-C. Constraining mid to late Holocene relative sea level change in the southern equatorial Pacific Ocean relative to the Society Islands, French Polynesia. *Geochem. Geophys. Geosystems* **2014**, *15*, 2601–2615. [CrossRef]

48. Pirazzoli, P.; Montaggioni, L. Lithospheric deformation in French Polynesia (Pacific Ocean) as deduced from Quaternary shorelines. In Proceedings of the 5th International Coral Reef Congress, Tahiti, French Polynesia, 27 May–1 June 1985.

49. Mathe, D. *Etude Géotechnique Préalable, Mission G1—Phase Principes Généraux de Construction (Norme NF P 94-500 Version de Novembre 2013)*; Laboratoire de Travaux Publics de Polynesie: Papeete, Tahiti, French Polynesia, 2014.

50. Ayers, J.F. *Groundwater Flow Dynamics Beneath Atoll Islands*; IAHS-AISH Publication: Wallingford, UK, 1998; pp. 397–404.

51. Briggs, M.A.; Cantelon, J.A.; Kurylyk, B.L.; Kulongoski, J.T.; Mills, A.; Lane, J.W. Small atoll fresh groundwater lenses respond to a combination of natural climatic cycles and human modified geology. *Sci. Total. Environ.* **2021**, *756*, 143838. [CrossRef]

52. Maréchal, J.-C.; Hakoun, V.; Corbier, P. Role of Reef-Flat Plate on the Hydrogeology of an Atoll Island: Example of Rangiroa. *Water* **2022**, *14*, 2695. [CrossRef]

53. Breier, J.A.; Breier, C.F.; Edmonds, H.N. Detecting submarine groundwater discharge with synoptic surveys of sediment resistivity, radium, and salinity. *Geophys. Res. Lett.* **2005**, *32*. [CrossRef]

54. Day-Lewis, F.D.; White, E.A.; Johnson, C.D.; Lane, J.W.; Belaval, M. Continuous resistivity profiling to delineate submarine groundwater discharge—Examples and limitations. *Geophysics* **2006**, *25*, 724–728. [CrossRef]

55. Jackson, P.D.; Briggs, K.B.; Flint, R.C.; Holyer, R.; Sandidge, J. Two- and three-dimensional heterogeneity in carbonate sediments using resistivity imaging. *Mar. Geol.* **2002**, *182*, 55–76. [CrossRef]

56. Binley, A.; Slater, L. *Resistivity and Induced Polarization: Theory and Applications to the Near-Surface Earth*; Cambridge University Press: Cambridge, UK, 2020.

57. Singha, K.; Johnson, T.; Day-Lewis, F.; Slater, L. *Electrical Imaging for Hydrogeology*; No. PNNL-SA-159896; Pacific Northwest National Laboratory (PNNL): Richland, WA, USA, 2022.

58. LaBrecque, D.J.; Yang, X.; Hermans, T.; Kemna, A.; Terry, N.; Comas, X.; Reeve, A.S.; Schäfer, K.V.R.; Yu, Z.; Mellors, R.; et al. Difference Inversion of ERT Data: A Fast Inversion Method for 3-D In Situ Monitoring. *J. Environ. Eng. Geophys.* **2001**, *6*, 83–89. [CrossRef]

59. Jackson, P.D.; Pearce, J.; Jarrard, R.; Pigram, C. Resistivity/Porosity/Velocity Relationships from Downhole Logs: An Aid for Evaluating Pore Morphology. In Proceedings of the Ocean Drilling Program, Townsville, Australia, 4 August–11 October 1990.

60. Pain, A.J.; Martin, J.B.; Young, C.R.; Valle-Levinson, A.; Mariño-Tapia, I. Carbon and phosphorus processing in a carbonate karst aquifer and delivery to the coastal ocean. *Geochim. Cosmochim. Acta* **2020**, *269*, 484–495. [CrossRef]

61. Jackson, P.D.; Taylor Smith, D.; Stanford, P.N. Resistivity-porosity-particle shape relationships for marine sands. *Geophysics* **1978**, *43*, 1250–1268. [CrossRef]

62. Gischler, E.; Hudson, J.H.; Humblet, M.; Braga, J.C.; Schmitt, D.; Isaack, A.; Eisenhauer, A.; Camoin, G.F. Holocene and Pleistocene fringing reef growth and the role of accommodation space and exposure to waves and currents (Bora Bora, Society Islands, French Polynesia). *Sedimentology* **2019**, *66*, 305–328. [CrossRef]
63. Cabioch; Camoin; Montaggioni. Postglacial growth history of a French Polynesian barrier reef tract, Tahiti, central Pacific. *Sedimentology* **1999**, *46*, 985–1000. [CrossRef]
64. Weij, R.; Reijmer, J.J.G.; Eberli, G.P.; Swart, P.K. The limited link between accommodation space, sediment thickness, and inner platform facies distribution (Holocene–Pleistocene, Bahamas). *Depos. Rec.* **2019**, *5*, 400–420. [CrossRef]
65. Ayers, J.F.; Vacher, H.L. Hydrogeology of an Atoll Island: A Conceptual Model from Detailed Study of a Micronesian Example. *Groundwater* **1986**, *24*, 185–198. [CrossRef]